Available online at www.sciencedirect.com

SCIENCE DIRECT®

Polymer 46 (2005) 10484–10492

polymer

www.elsevier.com/locate/polymer

Studies on the properties of a new hybrid materials containing chain-extended urea and SiO_2–TiO_2 particles

Shao-Rong Lu[a,b,*], Hai-Liang Zhang[b], Cai-Xian Zhao[b], Xia-Yu Wang[b]

[a]*Key Laboratory of Nonferrous Metal Materials and New Processing Technology (Guilin of Institute Technology), Ministry of Education, Guilin, Guangxi 541004, People's Republic of China*

[b]*Institute of Polymer Science, Xiangtan University, Xiangtan, Hunan 411105, People's Republic of China*

Received 3 January 2005; received in revised form 9 August 2005; accepted 10 August 2005
Available online 26 August 2005

Abstract

EP/SiO_2–TiO_2 hybrid materials, which contained chain-extended urea, were prepared through sol–gel process of triethoxylsilyl functionalized polyethylene oxide (PEO)-2000, i.e. chain-extended urea –PEO–$[Si(OC_2H_5)_3]_2$, tetraethoxysilane (TEOS) and tetrabutyltitanate (TBT) using HCl as catalyst. The PEO–$[Si(OC_2H_5)_3]_2$ was obtained by endcapping PEO-2000 with tolylene 2,4-diisocyanate (TDI), followed by a reaction with 3-aminopropyltriethoxylsilane (WD-50). The chemical structure of the products was confirmed by IR measurements. The curing reactivity, the apparent activation energy (E_a), and the mechanical properties of composites such as impact strength, flexural strength, dynamic mechanical thermal properties were investigated. The results showed that the addition of PEO–$[Si(OC_2H_5)_3]_2$ to epoxy resin and DDS curing system could reduce the apparent activation energy (E_a) of the curing reaction and accelerate the curing reaction. In addition, the glass transition temperatures were little alteration, while the modulus maintained high value, and the impact strength was enhanced by 2–3 times compared with that of the neat epoxy. The morphological structure of impact fracture surface and the surface of the hybrid materials were observed by scanning electron microscope (SEM) and atomic force microscopy (AFM), respectively.

Keywords: Hybrid materials; EP/SiO_2–TiO_2; Chain-extended urea

1. Introduction

Over the past decade, the synthesis and characterization of inorganic–organic hybrid materials containing a mixture of inorganic and organic components by the sol–gel process have received considerable attention [1–6]. The incorporation of organic components would expectantly impart flexibility to the inorganic glass, and the introduction of inorganic components would improve the hardness and modulus of the organic compounds. This multicomponent system could thus, show some characteristics of the inorganic glassy network and some properties of the organic species [7].

In general, two approaches are usually utilized to prepare organic–inorganic hybrid materials. In the first case, the covalent bonds between the polymer and ceramics (e.g. silica or titania, etc.) are formed. Polymers having $-Si(OR)_3$ groups at the end or in the pendant groups are subjected to hydrolysis together with $Si(OR)_4$ in a homogeneous reaction system. Intermediate species of silanol groups derived from $Si(OR)_4$ and $-Si(OR)_3$ in polymers are condensed with each other to produce homogeneous materials containing chemically bonded components. The other case is the three-dimensional network of silica (or ceramics), which dispersed in polymer molecules and formed by a hydrogen bond between the basic group of the hydrogen-acceptor function in the polymer and the silanol group ($\equiv SiOH$) of the intermediate species from $Si(OR)_4$ [8,9].

Epoxy resin is one of the most important thermosetting polymer materials. It has many excellent properties, such as high thermal stability, adhesion, mechanical and electrical properties, and is widely used in coating, adhesives, castings, etc. However, it is well known that the commonly used epoxy resin is generally rather brittle when cured with stoichiometric amount of common curing agents such as

---

[*] Corresponding author. Address: Institute of Polymer Science, Xiangtan University, Xiangtan, Hunan 411105, People's Republic of China. Tel.: +86 773 5896672; fax: +86 773 5896671.
E-mail address: lushaor@163.com (S.-R. Lu).

0032-3861/$ - see front matter © 2005 Elsevier Ltd. All rights reserved.
doi:10.1016/j.polymer.2005.08.029

Table 1
Sample preparation and composition

Sample	EP (g)	TBT (g)	TEOS (d)	PEO–$[Si(OC_2H_5)_3]_2$ (g)	SiO_2–TiO_2[a] (wt%)	Impact strength (kJ/m^2)
0	100	0	0	0	0	11.58
1	100	0.65	2.0	20	0.92	21.46
2	100	1.30	4.0	20	1.57	33.42
3	100	1.95	6.0	20	2.21	30.71
4	100	2.60	8.0	20	2.86	28.64
5	100	3.25	10.0	20	3.45	23.18
6	100	1.30	4.0	10	1.43	27.62
7	100	1.30	4.0	15	1.52	29.30
8	100	1.30	4.0	25	1.63	30.75

Preparation condition: $[H_2O]$:[TEOS + TBT] = 1:1, [HCl]:[TEOS + TBT] = 0.05 (mol. rate).

[a] Silica and titania contents were calculated theoretically.

aliphatic or aromatic polyamides, dicarboxylic acids, anhydrides, boro trifluoride, and tertiary amines, because of its highly crosslinked structure. Its poor fracture toughness greatly limits the use of this resin in structure applications. However, the improvement of toughness for the cured epoxy resin is highly desirable to overcome their brittleness. One of the methods is by incorporating rigid, or reactive rubbery particles, or both of them [10–12]. However, modification by the addition of rubber is usually at the expense of T_g and modulus. Another way is by incorporating tough, high performance, and thermal stable engineering plastics, such as polyethersulfones [13] and polyetherimide [14]. Liquid crystalline polymers as fillers are also used to improve the toughness recently [15]. All the approaches mentioned above have been achieved by improving in toughness.

It is well known that it is difficult to maintain high T_g and modulus of epoxy resin when increasing its impact strength. For this reason, we synthesized a new type of reactive chain-extended urea –PEO–$[Si(OC_2H_5)_3]_2$ containing both rigid inorganic particle and flexible spacer to modify the DDS cured epoxy resin system. The rigid particle is aimed to keep the high modulus and good thermal properties, while the flexible chains are used to improve the toughness.

2. Experimental

2.1. Materials and measurements

Epoxy resin (diglycidyl ether of bisphenol A DGEBA(E-51), WEP = 196, purchased from Yueyang Chemical Plant, China, without further purification). WD-50 was purchased from Chemical Reagent Co. of Wuhan University, China, and was purified by distillation before use. PEO-2000 was of analytical grade and carefully got rid of water before use. Other reagents were purified by conventional methods. Tetraethoxysilane (TEOS) and tetrabutyltitanate (TBT) (both chemical reagent grade) were ordered from Xilong Chemical Fractory, Guangdong, China. Toluenediisocyanate (TDI)(80/20) was purified by distillation under vacuum, 4,4′-diaminodiphenylsulphone (DDS) purchased from Shanghai Chemical Reagent Company, China, with a molecular mass of 248.31 and purity > 96% according to the supplier.

Fourier transformed infrared spectroscopy (FTIR) was recorded between 4000 and 400 cm^{-1} on a Perkin–Elmer 1710 spectrophotometer using KBr pellets at room temperature. The crystal behaviour of the EP and EP/SiO_2–TiO_2 material was analyzed by X-ray diffractometry (XRD:D/max-RB, Japan). UV–vis spectra were measured on a shimadzu UV-265 spectrophotometer. The impact strength was measured on a tester of type XJJ-5, which is with no notch in the specimen according to China National Standard GB1043-79. The flexural strength was examined on an electron omnipotence tester of type RGT-5 (REGER instrument company, Shenzhen, China). Testing machine according to China National Standard GB1040-92. All the presented results are average of five specimens. Differential scanning calorimetry (DSC) was carried out using NETZSCH DSC204 at a heating rate of 5, 10, 15, 20 K/min, respectively. Dynamic mechanical analysis (DMA) was determined using a linear rheometer (Rheometrics 902–50010 dynamic mechanical analyzer, was made with a TA instruments) in a three point bending, at a frequency of 1 Hz from −100 to 220 °C at a heating rate of 5 °C/min. Atomic force microscopy (AFM) was carried out using AJ-IIIa (Shanghai AJ Nano-Science Development Co. Ltd, China). The scan rate is 2.00061 Hz, scan size is 5.00061, the number of sample is 256.

2.2. Preparation of sol–gel precursor PEO–$[Si(OC_2H_5)_3]_2$

Into a three-necked round-bottomed flask, which was equipped with a stirrer, an N_2 inlet and a cooler. TDI (7.0 ml) dissolved in proper amount of acetone was added. Then an excessive amount of PEO-2000 (PEO-2000:TDI = 2:1) was dropped into the flask with 1 h. The solution was stirred for additional 17 h at 30 °C, the yellow solution was obtained. Terminal of reaction was confirmed by determination of the isocyanate group content by means of titration. Then amount of WD-50 and acetone mixture were dropped

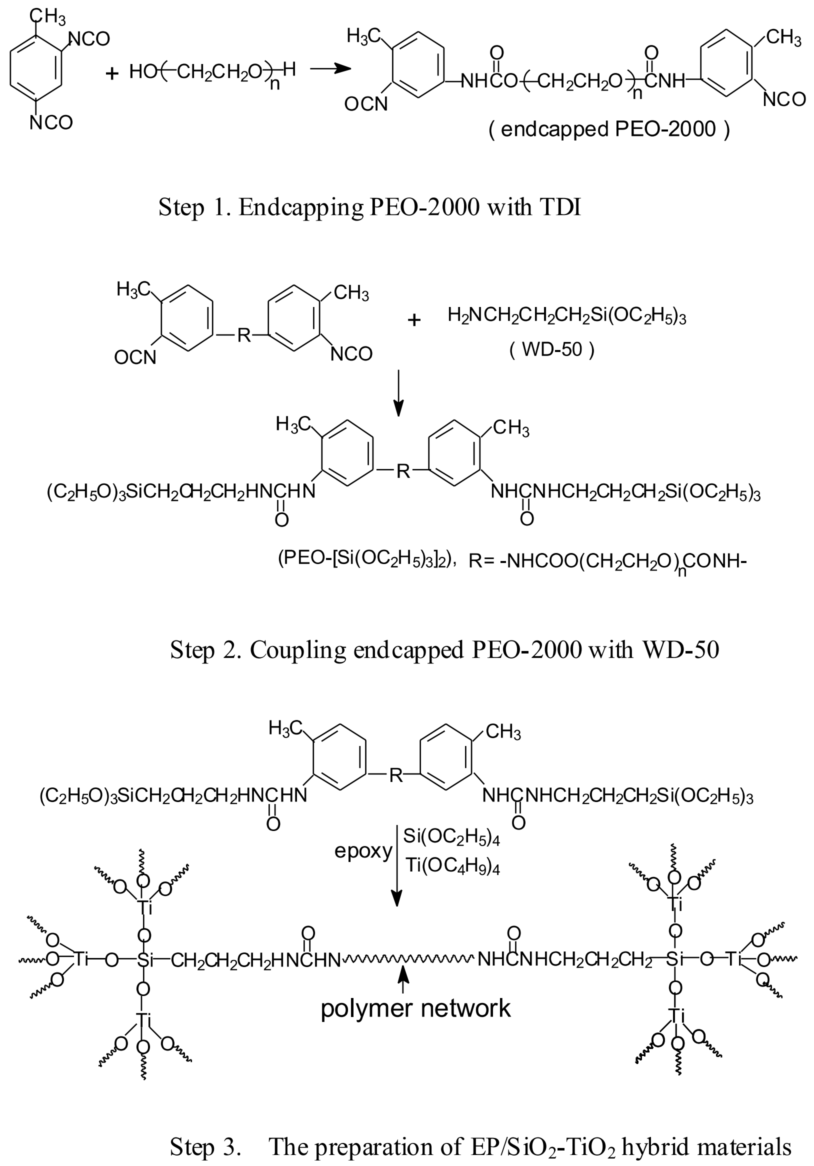

Scheme 1. The step reactions for preparing EP/SiO_2–TiO_2 hybrid materials; step 1, endcapping PEO-2000 with TDI; step 2, coupling endcapped PEO-2000 with WD-50; step 3, the preparation of EP/SiO_2–TiO_2 hybrid materials.

into above solution within 3 h, stirred at 30 °C for additional 1 day. The final precursor PEO–$[Si(OC_2H_5)_3]_2$ was obtained by getting rid of acetone under vacuum at 50 °C.

2.3. Preparation of sol–gel precursor for hybrid materials

In a 250 ml round-bottom flask, about 100 g epoxy resin, and an appropriate amount of PEO–$[Si(OC_2H_5)_3]_2$, TBT, TEOS, hydrochloric acid, distilled H_2O and THF were introduced. After vigorous stirring for 30 min, the mixture became homogenous. Then, the solution was transferred into a 250 ml beaker and covered with parafilm to allow the evaporation of small molecules for a few days, and the epoxy/silica–titatia hybrid precursors were obtained according to the recipe listed in Table 1.

2.4. Curing procedure

A mixture of epoxy/silica–titatia hybrid precursor and a stoichiometric amount of DDS (30 g/100 g of epoxy resin) was degassed in vacuum at 130 °C for about 30 min. The resulting mixture was then cast into a preheat mold coated with silicone resin. All samples were cured at 130 °C for 2 h, 170 °C for 2 h and 190 °C for 2 h.

3. Results and discussion

3.1. Characterization of hybrid materials

As mentioned in Section 2, preparation of hybrid materials included three steps. The possible step reactions are shown in Scheme 1.

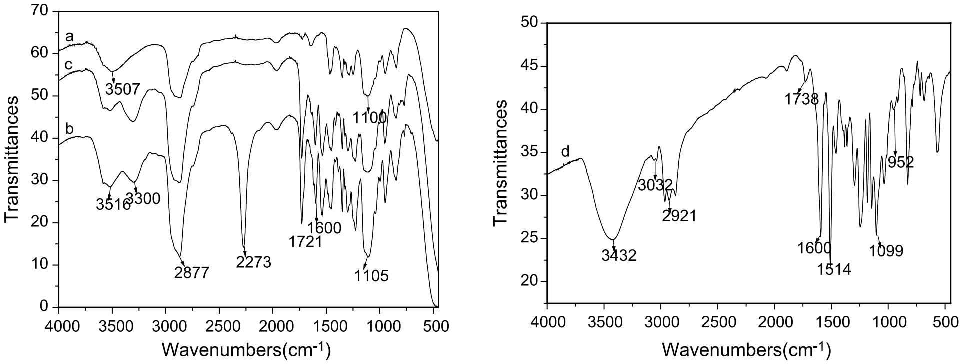

Fig. 1. The FTIR spectra of (a) PEO-2000; (b) endcapped PEO-2000; (c) PEO–[Si(OC_2H_5)$_3$]$_2$; (d) EP/SiO_2–TiO_2 hybrid material.

Step 1 was hydrogen shift reaction between tolylene 2,4-diisocyanate and PEO-2000, resulting in urethane coupling between their molecules and endcapped PEO-2000 as the product. Since the molar ratio of them was 2:1, so mainly the contrapuntal –NCO groups on TDI took part in the reaction, with the neighboring groups remaining unreacted. Step 2 is a coupling reaction of WD-50 with the endcapped PEO-2000. In this step, –NH_2 groups of WD-50 reacted with –NCO groups of endcapped PEO-2000, forming carbamido linkage –PEO–[Si(OC_2H_5)$_3$]$_2$, which contains –Si(OC_2H_5)$_3$ and –NH– groups. Step 3 is the preparation of EP/SiO_2–TiO_2 hybrid materials. In this step, it concludes two steps, in the first step, epoxy, PEO–[Si(OC_2H_5)$_3$]$_2$, Si(OC_2H_5)$_4$, Ti(OC_4H_9)$_4$ and distilled water were hydrolyzed by using hydrochloric acid as catalyst in THF, resulting in precursor for hybrid materials. The another step is a curing reaction of the precursor of hybrids and DDS curing agent, in this process, –NH– groups of PEO–[Si(OC_2H_5)$_3$]$_2$ and –NH_2 groups of DDS reacted with oxirane of epoxy forming polymer network, and the covalent bonding Si–O–Ti was also formed by hydrolysis/condensation between Ti–OC_4H_9, Si–OC_2H_5 and –Si(OC_2H_5)$_3$ groups.

Fig. 1 shows the FTIR spectra of (a) PEO-2000 (b) endcapped PEO-2000 (c) PEO–[Si(OC_2H_5)$_3$]$_2$ (d) EP/SiO_2–TiO_2 hybrid material. In (a), a distinct absorption peak at ~1100 cm^{-1} is in the region of –C–O–C stretching for ether groups and the peak at 3507 cm^{-1} belongs to –OH group. In (b) the peak at ~2270 cm^{-1} confirms the existence of –NCO groups. In (c) the peak at ~2270 cm^{-1} disappeared, while the peak at ~1100 cm^{-1}increased since the –C–O–C stretching over lapped with Si–O–C stretching band. Absorption bands at ~1721 cm^{-1} in both (b) and (c) were mainly due to –C=O asymmetric stretching from urethane groups. In (d) the peak at 3432 cm^{-1} is a result of the Ti–OH and the Si–OH group [16] and the peak at 1099 cm^{-1} is assigned to the Si–O–C and Ti–O–C [17]. There was also the broad absorption at lower wavenumber region. Especially 1100–920 cm^{-1}is assigned to the Si–O–Si and Si–O–Ti, and the peak at 950 cm^{-1} is attributed to Si–O–Ti bonds [18].

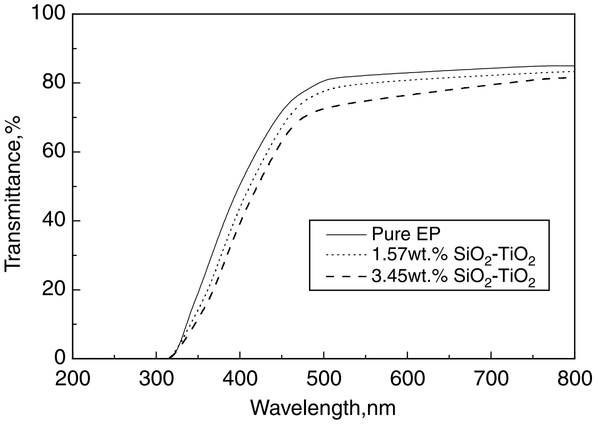

Fig. 2. The transparency curves of the pure EP and EP/SiO_2–TiO_2 hybrid films.

3.2. Optical behavior of the EP/SiO_2–TiO_2 hybrid films

The appearances of the EP/SiO_2–TiO_2 hybrid films with different EP/SiO_2–TiO_2 contents are shown in Fig. 2. It can be seen that the transparency of the EP/SiO_2–TiO_2 hybrid films are almost unchanged by the addition of the TEOS and TBT. This is because PEO–[Si(OC_2H_5)$_3$]$_2$ hydrolyzes to form silanol groups that can polycondense with the hydrolysis product of TEOS and TBT, which leads to increased compatibility with epoxy. This factor leads to smaller SiO_2–TiO_2 particles size and well dispersion of the SiO_2 and TiO_2 in the epoxy matrix.

3.3. Mechanical performance

The most common approach used to enhance the toughness of epoxy resin is to add a softer second phase to epoxy resin [19]. The dispersed rubber phase plays an important role in the toughness improvement of the material. Rubber particles acting as stress concentrators, which allows the matrix between the particles to undergo both shear and craze deformation. The impact resistance property of the cured epoxy with different amount of PEO–[Si(OC_2H_5)$_3$]$_2$ and SiO_2–TiO_2 contents were evaluated on a charpy impact testing machine, and results are listed in

Table 1. It is very clear that the addition of the chain-extended ureas significantly improves the toughness of the cured epoxy resin. In this study, the chain-extended ureas with flexible spacers and SiO_2–TiO_2 nanoparticles act as a softer second phase and stress concentrators.

Table 1 also shows the impact toughness of the composites increases with SiO_2–TiO_2 contents. Since unnotched charpy impact strength reflects the energy consumed before fracture, and SiO_2–TiO_2 nanoparticles in the composites are able to induce plastic deformation of the surrounding matrix polymer to a certain extent under the condition of high strain rate. The results of the Table 1 show the impact strength seems to be effective already at low SiO_2–TiO_2 contents of 0.92 wt% and reaches the highest level for SiO_2–TiO_2 contents about 1.57 wt%. Since nanoparticles act as strong stress concentrators, it may induce epoxy matrix yielding deformation and resistance to crack propagation [20], under lower particle contents, the dispersion of the particles in the epoxy matrix was good enough the impact strength increased as increasing of the SiO_2–TiO_2 contents. However, aggregation of the particles became obvious when the particle content reached 3.45 wt%. Since large particles can act as crack initiation sites and high aspect ratio particles are able to induce large stress concentrations near their edges. In higher SiO_2–TiO_2 contents, the impact energy decreases gradually. However, it remains well above the performance of the pure epoxy.

The flexural strength of microparticle filled composites is known to reduce with rising filler content for the bonding between the filler particles and the matrix is poor [21,22]. If the bonding between fillers and matrix is instead strong enough, the yield strength of a particulate composite can be higher than that of the matrix polymer [23]. From Fig. 3, it may be seen that both flexural strength and modulus increase with SiO_2–TiO_2 contents (20% PEG–$[Si(OC_2H_5)_3]_2$) increasing. That means the interaction between SiO_2–TiO_2 nanoparticles and epoxy matrix so strong that the nanoparticles are able to carry the applied load. The results of experiment indicated when the SiO_2–TiO_2 content is 2.21 wt%, the flexural strength and modulus of the composite were 80.9% higher than that of epoxy resin (1.36 GPa) and 29.7% higher than that of the epoxy resin (85.3 MPa), respectively. This increase suggests that the nanoparticles are able to introduce additional mechanisms of failure and energy consumption without blocking matrix deformation, and may induce matrix yielding under certain conditions and may furthermore act as stoppers to crack growth by pinning the cracks [24]. Nevertheless, if the fillers exceed 2.21 wt%, the failure strain undergoes a slight decay, such as reduction proposes that the large number of fillers now dominate, and they reduce the matrix deformation by restraining mechanically.

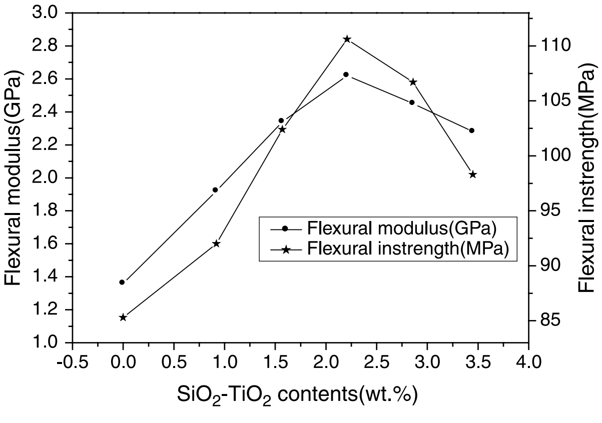

Fig. 3. The relation between SiO_2–TiO_2 contents and flexural strengths, flexural modulus.

3.4. XRD analysis

XRD patterns for reagent grade SiO_2, pure EP and EP/SiO_2–TiO_2 hybrid material are given in Fig. 4. Fig. 4(a) shows that the peaks are very sharp, which belongs to crystallite structure. The XRD patterns of Fig. 4(b) and (c) display only a very broad hump peak, the contact angle of (b) and (c) were around 2θ ranging between 10 and 30°, originating from amorphous phase of epoxy resin. This result indicates that SiO_2 and TiO_2 do not form sufficiently large clusters for XRD during epoxy curing process. Thus, the introduction of SiO_2 and TiO_2 disrupt the epoxy intermolecular, regularity.

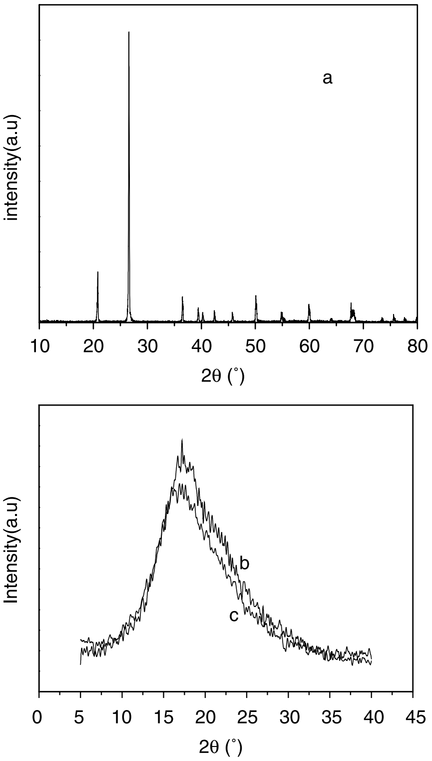

Fig. 4. X-ray diffraction patterns of (a) reagent grade SiO_2; (b) pure EP; (c) EP/SiO_2–TiO_2 hybrid material.

Table 2
DSC peak temperature (K) for the curing system at different heating rate

No.	Formulation	DSC peak temperature (K)			
		5 K/min	10 K/min	15 K/min	20 K/min
0	E-51/DDS = 100/30	479	501	514	522
1	E-51/DDS/PEO–$[Si(OC_2H_5)_3]_2$ = 100/30/5	456	478	490	499
2	E-51/DDS/PEO–$[Si(OC_2H_5)_3]_2$ = 100/30/10	450	470	483	493
3	E-51/DDS/PEO–$[Si(OC_2H_5)_3]_2$ = 100/30/15	442	461	475	484
4	E-51/DDS/PEO–$[Si(OC_2H_5)_3]_2$ = 100/30/20	438	457	470	480
5	E-51/DDS/PEO–$[Si(OC_2H_5)_3]_2$ = 100/30/25	435	454	465	478

3.5. Reactivity of the curing system

Applying DSC data has been a common analytical technique to determine kinetics of curing process. And the DSC peak temperatures are presented in Table 2. And the temperature peaks (T_p) of DSC at different the heating rate is shown in Table 2. DSC peak temperature (T_p) for the neat epoxy is as high as 501 K, However, DSC peak temperature (T_p) of containing 25% PEO–$[Si(OC_2H_5)_3]_2$ decrease to 454 K at the same heating rate. The decrease of DSC peak temperature reveals that the addition of PEO–$[Si(OC_2H_5)_3]_2$ can accelerate the curing reaction between epoxy and DDS greatly. And reactive process can be described by the activation energy.

The Kissinnger evaluation method is performed to determine the activation energy prior to identifying other kinetic parameters [25]. This method shows that the relationship between DSC peak temperature (T_p) and the heating rate K is of the following form: $\ln K = \ln A - (E_a/RT_p)$, where R is universal gas constant, T_p is temperature, E_a is activation energy and A is pre-exponential factor. A plot of $\ln K$ against $1/T_p$ should be linear with slope $= -E_a/R$. The data in Table 2 are plotted in this way in Fig. 5 and good linearity is obtained. The kinetic data derived from the plots are given in Table 3.

It can be seen from Table 3 that the curing activity of the E-51/PEO–$[Si(OC_2H_5)_3]_2$/DDS systems enhanced for the apparent activation energy of curing reaction decrease from 67.8 kJ/mol for the neat epoxy system to 55–60 kJ/mol. The curing reaction mechanism of E-51/PEO–$[Si(OC_2H_5)_3]_2$/

Table 3
Kinetic data of the curing systems determined by Kissinger's method

No.	E_a (kJ/mol)	ln A	Correlation coefficient, R
0	67.8	18.63	−0.99903
1	60.7	17.62	−0.99896
2	59.5	17.51	−0.99972
3	58.7	17.58	−0.99943
4	57.7	17.45	−0.99925
5	55.8	17 .46	−0.99825

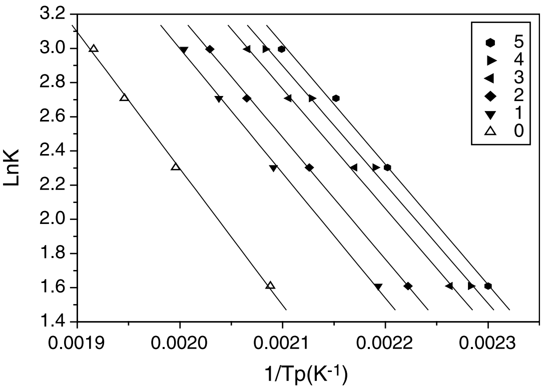

Fig. 5. Dependence of ln K on $1/T_p$ for the curing systems.

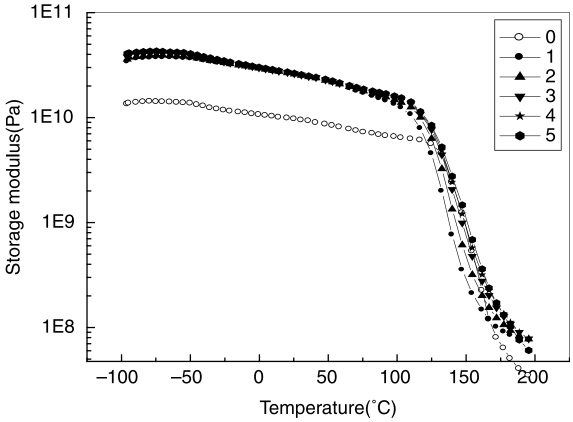

Fig. 6. Modulus vs. temperature for hybrid materials.

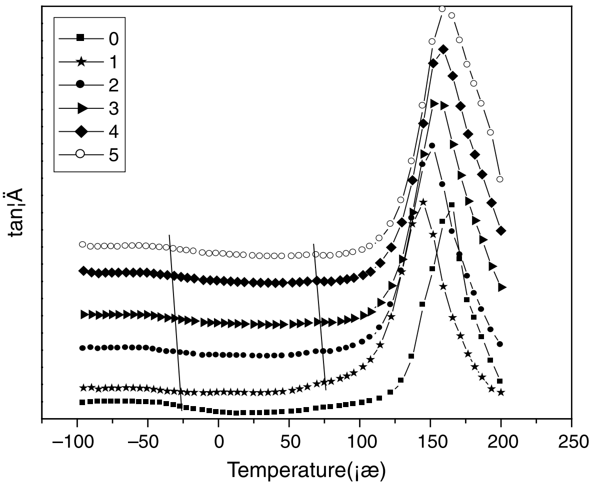

Fig. 7. Mechanical loss vs. temperature for hybrid materials.

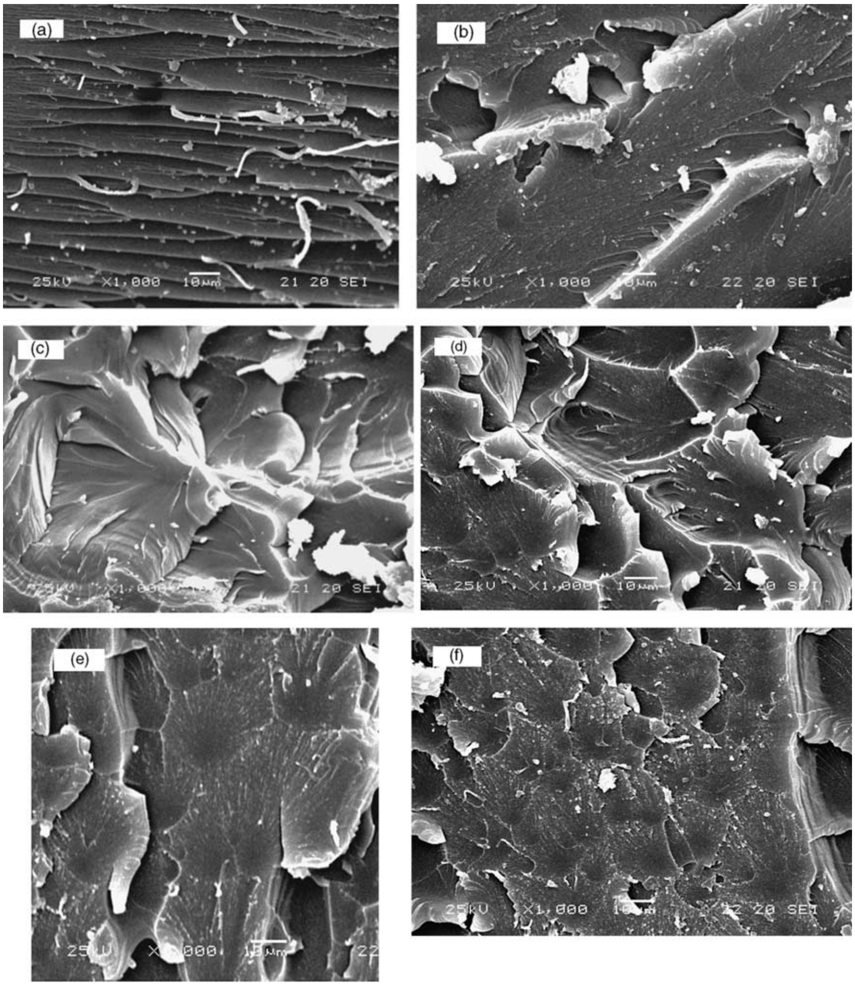

Fig. 8. SEM of the fracture surface of the modified systems with different SiO_2–TiO_2 (wt%) (a) 0; (b) 0.92; (c) 1.57; (d) 2.21; (e) 2.86; (f) 3.45.

DDS system accelerated by PEO–$[Si(OC_2H_5)_3]_2$ is mainly divided into two reasons. First, the urea group of the PEO–$[Si(OC_2H_5)_3]_2$ can accelerate the curing reaction, this is confirmed by Zhang B L et al., who reported that the curing reaction mechanism of E-51/dicy system accelerated by ATU is attributed to the urea group [26]. Secondly, the hydroxyl group of the Si–OH and Ti–OH, which are hydrolyzed TEOS, TBT and PEO–$[Si(OC_2H_5)_3]_2$ can also reacts with epoxide group leads to accelerate curing reaction.

3.6. Dynamic mechanical properties of EP/SiO_2–TiO_2 hybrid materials

The temperature dependence of dynamic mechanical properties of the EP/SiO_2–TiO_2 hybrids containing different amount of silica and titania network are shown in Fig. 6. The dynamic elastic modulus of the EP/SiO_2–TiO_2 hybrids were 20% higher than that of the pure epoxy. Generally, dynamic modulus would be decreased with the addition of the flexible chain spacer. However, due to the EP/SiO_2–TiO_2 hybrid materials containing not only the flexible spacer but also the rigid SiO_2–TiO_2 particles, the high dynamic modulus could be maintained. The flexible spacers are aimed to improve impact strength, and the rigid SiO_2–TiO_2 particles is intended to retain high dynamic modulus and thermal properties of the EP/SiO_2–TiO_2 hybrid materials. The rigid SiO_2–TiO_2 particles played a great role in enhancing the high dynamic modulus of epoxy resin modified by PEO–$[Si(OC_2H_5)_3]_2$.

Fig. 7 shows the dynamic mechanical spectra for tan δ of the EP and EP/SiO_2–TiO_2 hybrids. Compared to the neat epoxy, the peak glass transition temperature (T_g) of EP/SiO_2–TiO_2 hybrids slightly decreased with the addition of 20% PEO–$[Si(OC_2H_5)_3]_2$, with rising SiO_2–TiO_2 contents, the peak glass transition temperature of EP/SiO_2–TiO_2 tends to move to high values, while the damping peak decreases. The increasing in T_g may be attributed to a loss in the mobility of chain segments of epoxy resin resulting from the SiO_2–TiO_2 particles/matrix interaction and impeded chain mobility. Besides α-transition, there appears α-relaxation at around 70 °C, which might be contributed by the addition of PEO–$[Si(OC_2H_5)_3]_2$ to the epoxy resin. It has been suggested by Ochi and Shimbo that β-relaxation observes

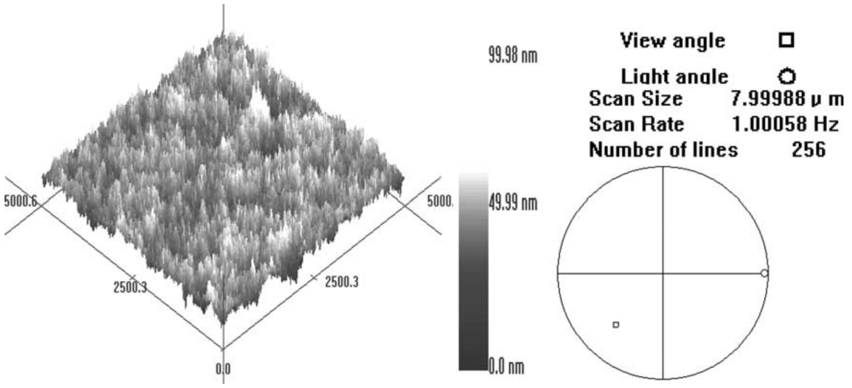

Fig. 9. AFM surface images of the SiO_2–TiO_2 composite specimen, The scan area is 5 μ×5 μm.

at about −40 °C in the amine-cured epoxy resin system is the contribution from the segment of –$CH_2CH(OH)CH_2N$–, while β-relaxation observes at about −70 °C is of the segment of –CH_2CH_2O– generated during the curing reaction [27,28]. From the above results, it can be inferred that the PEO–$[Si(OC_2H_5)_3]_2$, TEOS and TBT have been incorporated into the cross-linked epoxy resin network, which leads to the formation of phase-separation structure, this kind of structure is favorable to enhancement of impact strength.

3.7. Morphological structure of hybrids

The impact behavior of the modified system can be explained in term of morphology observed by SEM. The SEM microphotographs for the neat epoxy matrix is shown in (Fig. 8(a)). From the photograph, one can see the smooth glassy fractured surface with uniform crack direction in case of unmodified system. This indicates brittle behavior of the unmodified epoxy network, which accounts for its poor impact strength. As for the EP/SiO_2–TiO_2 composites (Fig. 8(b)–(f)), the fracture surfaces present holes and indentations and deep cracks, it can clearly be seen that the fracture stripes divert to different directions, indicating the characteristic of toughening facture. The results can be ascribed as two parts: First, it is matrix shear deformation as energy consuming mechanism in particulate filled epoxy resin, which has been reported by several authors [24]. Secondly, the phase separation started during the curing process. Overall, two reasons above lead to good impact resistance property of the cured epoxy resins modified with the PEO–$[Si(OC_2H_5)_3]_2$, TEOS and TBT.

The surface topography structure of the hybrid film (1.57% SiO_2–TiO_2 content) is characterized by AFM (Fig. 9). The film thickness is about 100 nm, the scan area is 5 μm×5 μm. From the micrograph, it can be seen that the SiO_2–TiO_2 particle size is about 20–50 nm, this indicates that SiO_2–TiO_2 'composite' particles is homogeneously and well disperse in the hybrid material matrix.

4. Conclusion

A transparent and homogeneous epoxy/silica–titania hybrids containing 0.92–3.45 wt% of silica–titania were obtained from epoxy, PEO–$[Si(OC_2H_5)_3]_2$, TEOS and TBT by using a sol–gel process. It was found that the chain-extended ureas containing PEO flexible spacers could act as effective toughening modifier for the epoxy resin, it could also decrease the apparent activation energy of curing reaction and accelerate the curing reaction. The impact strength of the cured systems modified with PEO–$[Si(OC_2H_5)_3]_2$ were three times higher than that of the neat epoxy. Furthermore, the addition of the TEOS and TBT could give high modulus and maintain the glass transition temperature at a slight changing. While the glass transition temperature are little changed, and the fracture surfaces of all modified systems display tough fracture feature.

Acknowledgements

Financial supports from the Natural Science Foundation of Guangxi province (No. 0447053) is gratefully acknowledged.

References

[1] Chiang P-C, Whang W-T. Polymer 2003;44:2249.
[2] Lee L-H, Chen W-C. Polymer 2005;46:2163.
[3] Xu H-Y, Kuo S-W, Lee J-S. Polymer 2002;43:5117.
[4] Matějka L, Dukh O, Kamišová H. Polymer 2004;45:3267.
[5] Liu Y-L, Su Y-H, Lai J-Y. Polymer 2004;45:6831.
[6] Jeng R-J, Chang C-C, Chen C-P. Polymer 2003;44:143.
[7] Novak BM. Adv Mater 1993;5:422.
[8] Saegusa T. Pure Appl Chem 1995;67:1965.
[9] Chujo Y. Polymeric materials encyclopedia. New York: Salamone; 1996. p. 4793.
[10] Maxwell D, Kinlock AJ, Yong RJ. J Mater Sci 1984;3:9.
[11] Yee AF, Pearson RA. J Mater Sci 1986;21:2462.
[12] He S-J, Shi K-Y, Bai J. Polymer 2001;42:9641.
[13] Iijima T, Tochimoto T, Tomoi M. J Appl Polym Sci 1991;43:1685.
[14] Jang BZ, Lian JY, Hwang LR, Shih WK. J Reinf Plast 1989;8:312.
[15] Carfagna C, Nicolais L. J Appl Polym Sci 1992;44:1465.

[16] Lee LH, Chen WC. Chem Mater 2001;13:1137.
[17] Zhang J, Wang BJ, Ju X, Liu T, Hu TD. Polymer 2001;42:3697.
[18] Sadlter Research Laboratories. Inorganics IR grating spectra. vols. 1–2. Philadelphia, PA: Sadlter; 1965. p. Y249k.
[19] Siebert AR. ACS Adv Chem Ser 1984;208:179.
[20] Wetzel B, Haupert F, Zhang MQ. Compos Sci Technol 2003;63:2055.
[21] Nicolais L, Narkis M. Polym Eng Sci 1971;11:194.
[22] Ahmed A, Jones FR. A review of particular reinforcement theories for polymer composites. New York: Chapman & Hall; 1995. p. 1–71.
[23] Wu CL, Zhang MQ, Rong MZ, Friedrich K. Compos Sci Technol 2002;62:1357.
[24] Roulin-Moloney AC. Fractography and failure mechanisms of polymers and composites. London: Elsevier Applied Science; 1986.
[25] Kissinger HE. Anal Chem 1957;11:1702.
[26] Zhang BL, Zhang HQ, You YC, Du ZJ. J Appl Polym Sci 1998;69:339.
[27] Ochi M, Shimbo M. J Polym Sci, Polm Phys Ed 1982;22:689.
[28] Ochi M, Shimbo M. J Polym Sci, Polm Phys Ed 1984;22:1461.